JOC The Journal of Organic Chemistry

Article

pubs.acs.org/joc

The Role of the Amino Acid-Derived Side Chain in the Preorganization of C_2-Symmetric Pseudopeptides: Effect on S_N2 Macrocyclization Reactions

Vicente Martí-Centelles,[†,‡] M. Isabel Burguete,[†] Carlos Cativiela,*[,‡] and Santiago V. Luis*[,†]

[†]Departamento de Química Inorgánica y Orgánica, ESTCE, Universitat Jaume I, E-12071 Castellón, Spain

[‡]Departamento de Química Orgánica, Instituto de Síntesis Química y Catálisis Homogénea (ISQCH), CSIC-Universidad de Zaragoza, E-50009 Zaragoza, Spain

Supporting Information

ABSTRACT: A family of pseudopeptidic macrocycles containing non-natural amino acids have been synthesized. The macrocyclization reaction has been studied experimentally and computationally, demonstrating the key role of both the amino acid side chain and the catalytic bromide anion. The bromide anion acts as an external template assisting the folding of the open-chain precursor in a proper conformation. Computations revealed that in the presence of the anion, the effect of the side chain on the energy barrier for the macrocyclization is very small. However, the effect on the conformational equilibria of the open-chain precursors is very important. Overall, the stabilization of those conformation(s) in which the two reactive ends of the open-chain intermediate are located at short distances from each other with the correct orientation is the critical parameter defining the success of the macrocyclization. The best yield was found for the compound containing cyclohexylalanine, for which the computationally-predicted most stable conformer in the presence of Br^- has a proper preorganization for cyclization. The remarkable agreement obtained between experiments and theory reveals that the computational approach here considered can be of great utility for the prediction of the behavior of other related systems and for the design of appropriate synthetic routes to new macrocyclic compounds.

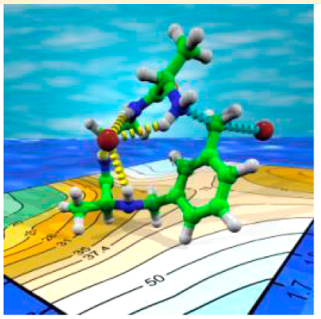

Minimalistic pseudopeptides

INTRODUCTION

The concept of preorganization is central to many, if not most, of the chemical functionalities that nature has developed. This is nicely illustrated in the case of enzymes.[1] Their unsurpassed catalytic activities depend on the presence in the active site of different functional groups belonging to amino acid moieties often situated very far away in the peptidic sequence.[2] Preorganization of such groups involves their proper location at the right distances and with the right orientation. When smaller molecules are considered, both in nature and for abiotic systems, preorganization is often approached through the preparation of cyclic structures.[3−5] The loss of conformational freedom associated with the cycle can provide a mechanism to fix the corresponding functional groups with the proper relative disposition.

The generation of many macrocyclic structures is not a simple matter, however, macrocyclization is favored when the corresponding open-chain precursors are themselves preorganized into a suitable folded conformation.[4−8] Different experimental evidences have been gathered both in the field of low-molecular-weight macrocycles and in the field of cyclic polymers, revealing that the distance between the two reactive ends in the open-chain intermediate experiencing the ring-closing reaction is a critical parameter determining the rate of the process.[9−12] In the absence of such preorganization, the cyclization reaction competes with oligomerization/polymerization processes, with the latter ones usually being favored unless high-dilution conditions are employed (Figure 1).[13,14] Thus, a detailed conformational analysis of both the expected macrocycle and the corresponding open-chain precursor can be a powerful tool to predict the potential outcome of a given macrocyclization.[13,15] As a matter of fact, macrocyclization reactions can be employed as a test to analyze conformational preferences on different systems.[16] This analysis, for instance, has been of importance in understanding polymerization processes involving bifunctional monomers. A second area in which this concept has been critical is the study of efficient approaches for the preparation of cyclopeptides and cyclic pseudopeptides, according to the importance of such structures for biomedical applications.[9,17,18]

In recent years, we have been involved in the preparation of different pseudopeptidic macrocyclic structures based on [1 + 1] or [2 + 2] cyclization processes, as the resulting families of compounds have been shown to display interesting properties.[19−21] These embrace the preparation of fluorescent sensors, leading to the development of intracellular pH sensors,

Received: October 15, 2013
Published: December 16, 2013

   dx.doi.org/10.1021/jo4022309 | J. Org. Chem. 2014, 79, 559−570

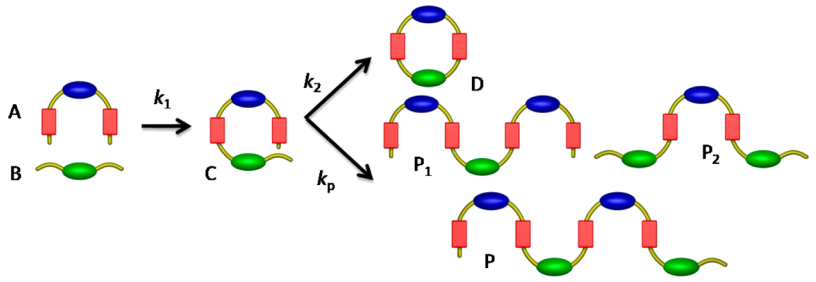

Figure 1. Competition between macrocyclization and oligomerization reactions.

minimalistic molecular machines, and new materials based on their self-assembling properties.

The successful synthesis of those macrocycles, which are based on a common C_2-symmetric scaffold (Scheme 1), has been carried out by favoring the correct folded conformation of the final open-chain intermediates in different ways. For simple [1 + 1] processes based on S_N2 reactions, the coexistence of intramolecular hydrogen bonds (particularly for compounds with shorter central spacers) and solvophobic effects plays an essential role,[22] while halide anions can act as efficient kinetic templates.[23−26] As, for the cases studied, halide anions are the leaving groups, this factor can act even in the absence of any added anion. In the case of [2 + 2] macrocyclizations based on reductive amination processes, the proper preorganization can be achieved through correct matching of the configurations of the chiral centers in the central spacer and the amino acid fragment or through the use of specifically designed organic anionic templates.[19]

Scheme 1. [1 + 1] Macrocyclic Structures Obtained from C_2-Symmetric Open-Chain Pseudopeptides

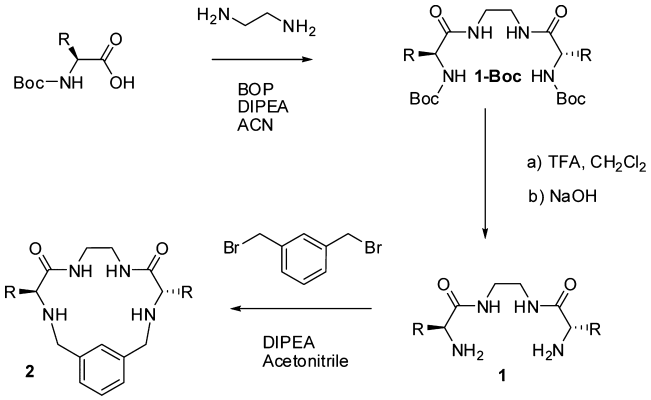

As reaching a preorganization suitable for cyclization involves achieving a U-folded conformation, it should be expected that the nature of the side chain of the component amino acid fragments would have an important effect in this regard. Many examples in the literature have revealed that the presence of specific amino acids or amino acid sequences is a key feature for peptides to adopt folded or helical arrangements.[16] For this purpose, the introduction of non-natural amino acids in the sequence is a common approach to modify the usual conformational trends and to force the presence of folding motifs.[27] Non-natural amino acids, on the other hand, can be synthesized through a variety of methods, allowing a large diversity of side chains to be introduced at the α and β positions to favor the appropriate conformational constrains.[28]

According to the former, we have designed and prepared a series of new C_2-symmetric pseudopeptides by considering a variety of potential amino acid side chains, and we have studied their behavior in [1 + 1] macrocyclization reactions based on S_N2 processes. The combination of experimental results and computational studies has been shown to be essential for the proper design of the selected systems and for an understanding of the effects observed, in particular the influence of the different structural features on the appropriate preorganization of the open-chain precursors. These results provide new insights into the preparation of macrocyclic peptides and related compounds, an important area of work because of the biomedical and pharmaceutical relevance of many of such structures. The difficulties associated with their synthesis often represent a limiting factor. The amino acid involved in the macrocyclization step is a key design vector, and understanding the specific effects of different side chains provides important parameters for this design.[29−31]

RESULTS AND DISCUSSION

The general structure of the pseudopeptidic macrocycles obtained by [1 + 1] cyclization processes contains three main elements of diversity: the central diamine spacer present in the open-chain starting pseudopeptide, the second spacer [usually a 1,3- or 1,4-bis(methylene)aryl fragment], and the component amino acid (Figure 2).

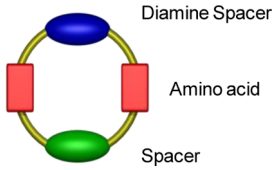

Figure 2. Structural variables in [1 + 1] macrocyclic compounds.

In order to simplify the study and highlight the role of the amino acid side chain, several constraints were considered. First, the alkylating agent to produce the cyclization from the open-chain compounds was fixed to be 1,3-bis(bromomethyl)-benzene. This is an standard alkylating agent used in previous experiments and thus allows an easy integration of results.[22,24] For the diamine spacer we considered exclusively aliphatic chains [$-(CH_2)_n-$]. Although [1 + 1] cyclization reactions have also been studied using diamines containing aromatic fragments,[24] the higher conformational flexibility of the aliphatic spacers could allow clearer observation of the contribution of the side chain to the conformational equilibria of the resulting open-chain pseudopeptides. In order to fix other constraints and to select the most appropriate materials for our work, various computational studies were initially

dx.doi.org/10.1021/jo4022309 | J. Org. Chem. 2014, 79, 559−570

carried out. In this regard, the structures considered for these studies are shown in Chart 1.

Chart 1. Pseudopeptidic Compounds Considered in This Work: the Constituent Amino Acids are (a) Phe, (b) Val, (c) Ala, (d) Aib, (e) Ac6c, (f) Cha, (g) Ile, (h) Leu, (i) Gly; PG = Protecting Group

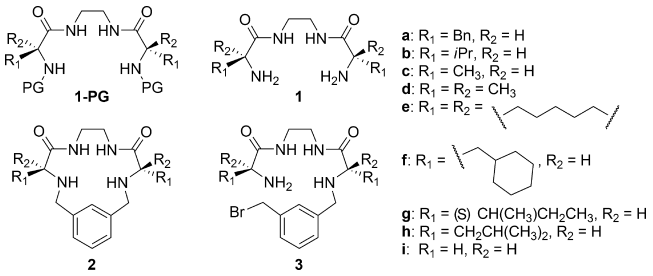

Conformational Studies. As considered above, the conformational behavior of the open-chain structures **3** has a direct influence on their reactivity. If the nitrogen atom of the reactive amine group has a proper orientation with regard to the carbon–halide group and is located a short distance away, the macrocyclization is favored. Otherwise, oligomerization takes place preferentially. Thus, the end-to-end distance averaged over all possible conformations must be analyzed to predict its reactivity to form a macrocyclic structure.[32,33] To analyze these intermediates, a conformational search was carried out using the Spartan'08 software to obtain the most stable conformer for each structure. This calculation was repeated at least three times until no variation of the Boltzmann-averaged nitrogen–carbon distance was observed. According to our previous results on the role of anions as kinetic templates,[24] the simulation was carried out for each amino acid in the absence and in the presence of the bromide anion (Figure 3).

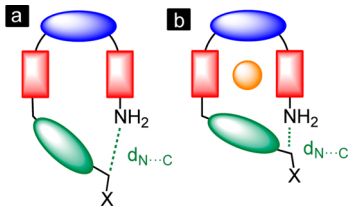

Figure 3. Schematic representation of the open-chain intermediates to be modeled in (a) the absence and (b) the presence of halide anion (denoted by the orange sphere).

The most important parameters to analyze in the optimized structures for reaction intermediates **3** obtained from the conformational searches are the N(amine)···C(halide) distance, the N(amine)···C(halide)–X angle, and the N(amine)···C(halide)–C(benzene ring)–X dihedral angle (where X denotes the halide). It seems clear, as has been shown for other systems, that a shorter N(amine)···C(halide) distance leads to a bigger probability for the reaction between the nitrogen atom and the carbon–halide, as the local concentration increases. However, it is important to take into consideration the fact that the presence of a short distance must be accompanied by a proper orientation of the two functional groups (Figure 4).

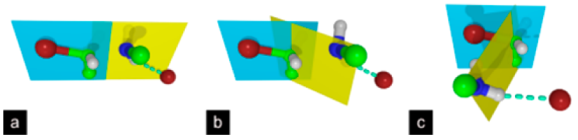

Figure 4. N(amine)···C(halide)–C(benzene ring)–X dihedral angle for the reactant interaction complex: (a) favorable orientation of 180°; (b) favorable orientation of 160°; (c) unfavorable orientation of 80°. Dark-red atoms, Br; green atoms, C; blue atom, N; blue plane, C(halide)–C(benzene ring)–X plane; yellow plane, N(amine)···C(halide)–C(benzene ring) plane.

Thus, reactive conformations must have low relative energy, a short N–C distance, a N···C–X angle in the 150–180° range, and a N···C–C–X dihedral angle ranging from 160° to 200° or from −200° to −160°. Accordingly, reactive conformations must be located in very limited regions of the overall conformational space. The ideal situation should be that in which the most stable conformers are located within the gray squares indicated in Figures 6 and 7 for all of the parameters considered.

This methodology can be illustrated for the case of the reaction intermediate **3f** derived from cyclohexylalanine. Figure 5 shows the geometries of the most stable conformers calculated for **3f** in (a) the absence and (b) the presence of the bromide anion.

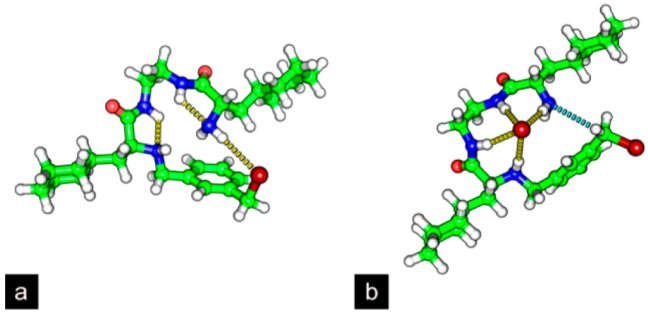

Figure 5. Representations of the MMFF-computed most stable conformers for the reaction intermediate **3f** in (a) the absence and (b) the presence of bromide anion.

The results of the MMFF[34] Monte Carlo conformational searches for **3f** in the absence of any added anion are presented in Figure 6. This provides a simple way to correlate the different structural parameters determined in the simulation of the reaction intermediate. According to the computational searches, the most stable conformers (red points in Figure 6) have short N···C distances but do not have dihedral angles that provide the correct orientation of the N atom relative to the C–Br bond. The calculated angle is not unique and varies from −100° to 175°, with a value near 0° for the most stable conformation (see Figure 6c).

The same simulation in the presence of the bromide anion (Figure 7) shows that the preferred conformation is completely different (Figure 5b), and only one stable conformation is present. This conformer (red dot in Figure 7) has the appropriate dihedral angle combined with a short N···C distance, which nicely correspond with the experimental results described below.

Thus, the presence of a Br^- anion acting as a kinetic template seems to be of paramount importance for the success of the macrocyclization. However, the side chain of the original amino

dx.doi.org/10.1021/jo4022309 | J. Org. Chem. 2014, 79, 559–570

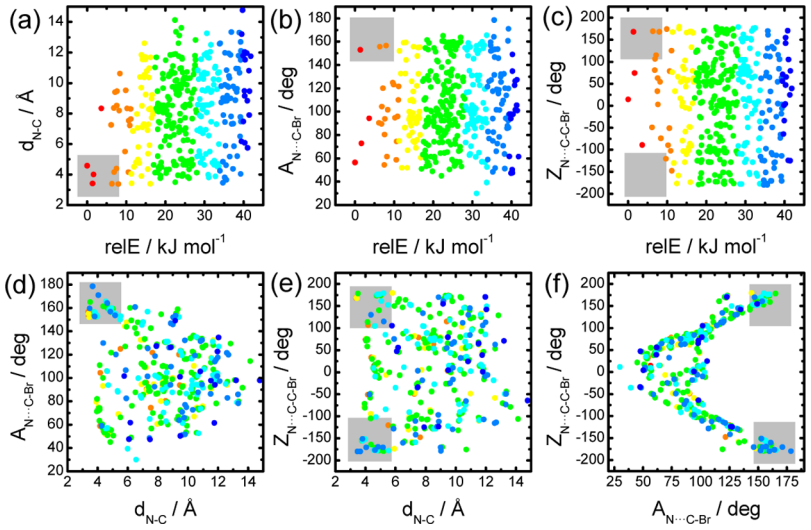

Figure 6. Representation of the conformational space for the reaction intermediate **3f** in the absence of any anion.

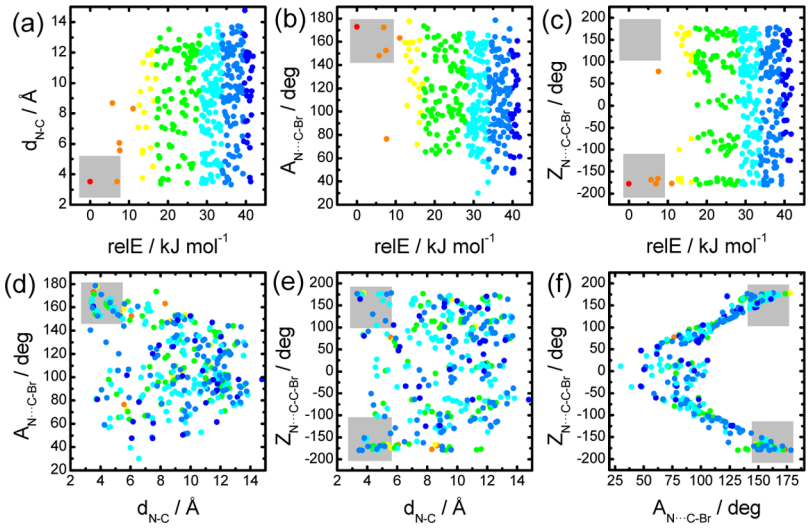

Figure 7. Representation of the conformational space for the reaction intermediate **3f** in the presence of Br^- anion.

acid also plays a critical role. This is illustrated by the data gathered in Figure 8, representing the Boltzmann-averaged C···N distances calculated for the intermediates **3** bearing different side chains. As can be observed, very large variations in this distance were calculated, and the effect of the anion can also be significantly different.

Experimental Kinetic Measurements. In order to carry out an experimental study of the corresponding macrocyclization processes, the required bis(amino amide)s **1** were synthesized as summarized in Scheme 1. All of the starting *N*-Boc-protected amino acids were commercially available. Their in situ activation with BOP followed by reaction with ethylenediamine afforded the *N*-Boc-protected open-chain compounds **1-Boc**.[35] After chromatographic purification, the Boc protecting groups were removed with trifluoroacetic acid to provide the expected derivatives **1** in good yields. Specific reaction conditions needed to be optimized for each particular case in view of the variety of amino acids considered. In particular, the reaction times required for quaternary amino acids were significantly longer because of their lower reactivities.

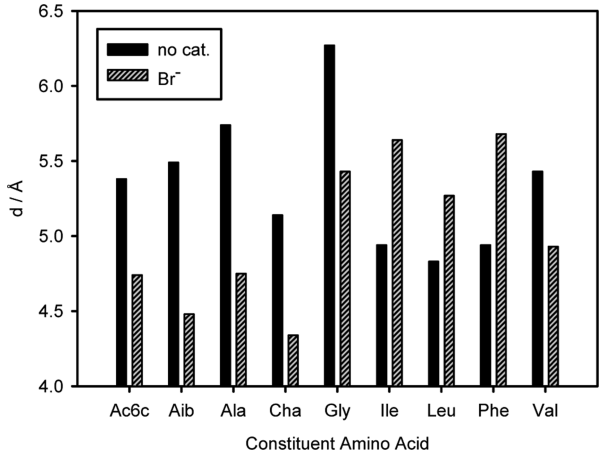

Figure 8. Representation of the average C···N distance for the reaction intermediates **3**. The amino acids are (left to right) Ac6c, Aib, Ala, Cha, Gly, Ile, Leu, Phe, and Val.

For the study of the macrocyclization reactions of open-chain pseudopeptides **1**, dry acetonitrile (ACN) was selected as the

dx.doi.org/10.1021/jo4022309 | J. Org. Chem. 2014, 79, 559−570

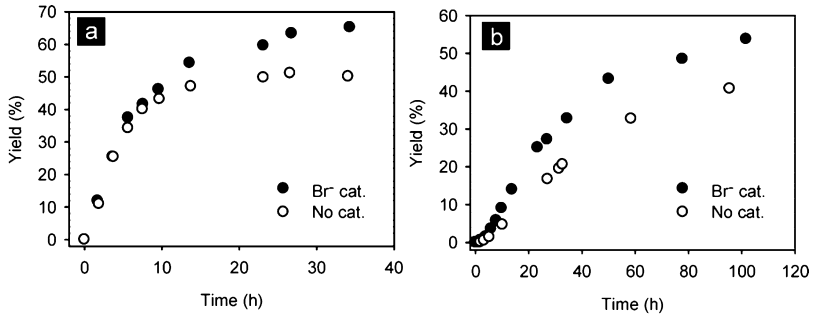

Figure 9. Kinetic curves for the formation of macrocycles (a) **2c** and (b) **2d** obtained in the presence (●) or absence (○) of bromide ion under otherwise identical conditions.

solvent, taking into consideration that its polarity seems to induce a favorable folding of the intermediates.[22] However, this precluded the use of the Gly derivative because of its low solubility in this solvent.

Initial kinetic experiments for the [1 + 1] macrocyclization were carried out with compounds **1d** (Aib) and **1c** (Ala). They were selected as models to compare the behavior of the derivative from a nonhindered natural amino acid (Ala) with that of the one resulting from the related quaternary non-natural amino acid (Aib). Macrocyclization experiments were performed using DIPEA (10 equiv), in the absence of any added anion or after the addition of 0.5 equiv of Br^- at the beginning of the reaction. The progress of the reaction was followed by ^{1}H NMR spectroscopy. DIPEA was selected as the base because it is a tertiary amine that is strong enough to avoid protonation of the amine groups of the different chemical species involved in the macrocyclization but not reactive toward any of the species participating in the process.[24] The results are represented in Figure 9. It can be seen that in agreement with the initial hypotheses, the bromide anion has a clear positive effect on the reaction rate and the final yield.

The interactions of both the open-chain and macrocyclic compounds with the bromide anion was confirmed by means of ^{1}H NMR experiments. The addition of increasing quantities of bromide anion produced a downfield shift of the signal of the amide group in both cases (Figure 10). This agrees with the existence of a hydrogen-bonding interaction of the amide with the bromide anion in the reactants and in the products, and therefore, this interaction should also exist in the transition state (TS).

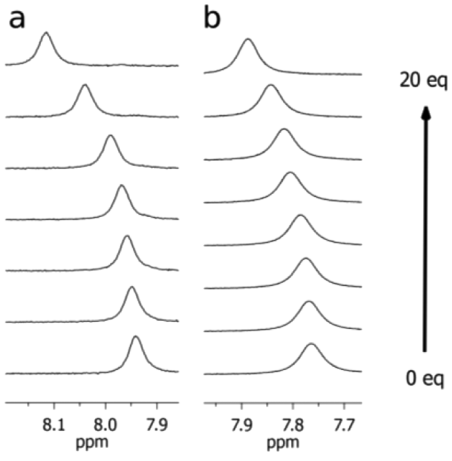

Figure 10. Variation of the amide signal in the ^{1}H NMR spectra of (a) **2d** and (b) **1d** with the addition of TBABr in ACN-d_3 at 25 °C.

On the basis of these results, the same experimental protocol was used to analyze the kinetics of the different macrocyclization reactions. Each reaction was carried out in an NMR tube, and each bis(amino amide) was allowed to react with 1 equiv of 1,3-bis(bromomethyl)benzene. In all cases, ACN-d_3 was used as the solvent, the temperature was kept at 25 °C, and 0.5 equiv of bromide anion was added at the beginning of the reaction. DIPEA (10 equiv) was used as the base and tetrakis(trimethylsilyl)silane (0.556 equiv) as the internal standard. ^{1}H NMR spectra were registered directly from the reaction mixture at different reaction times. The reactions were monitored for ca. 300 h for all of the compounds except those containing quaternary amino acids (Aib and Ac6c), for which monitoring was extended to ca. 800 h.

From the ^{1}H NMR spectra it was possible to obtain the concentrations of the macrocycle and the starting materials and detect the formation of byproducts. Figure 11 shows the overlapped ^{1}H NMR spectra for the process leading to **2f**. The increasing signals correspond to the macrocyclic product; the signal that disappears at 4.4 ppm is assigned to the benzylic protons of 1,3-bis(bromomethyl)benzene, and the one disappearing at around 7 ppm corresponds to the amide proton of the bis(amino amide). The signals of DIPEA move downfield, thereby confirming its protonation as the reaction takes place.

The formation of oligomeric/polymeric species was confirmed by mass spectrometry experiments. With ESI-MS it was possible to identify the starting material, the macrocyclic product, and some oligomers. Although the number of possible oligomers was high (see Figure S-1 in the Supporting Information) and their concentrations were always very low, the MS experiments allowed unambiguous detection and identification of several of them (see Figure S-2 in the Supporting Information).

Figure 12 gathers the different kinetic curves obtained from the ^{1}H NMR experiments. From these curves, a detailed kinetic analysis was carried out in order to determine the main kinetic parameters for each specific macrocyclization reaction.

To avoid overparametrization of the model, it was assumed that the kinetic constants for the S_N2 reactions that afford open-chain compounds (i.e., the first reaction step and the oligomerization/polymerization steps) are essentially identical (i.e., $k_1 = k_p$).[24,36] This provided a simple kinetic model to which the experimental kinetic data could be fitted. In this way, the corresponding kinetic parameters could be calculated. Figure 13a displays the expected time variation of the concentrations of the different species involved for **2f** obtained

dx.doi.org/10.1021/jo4022309 | J. Org. Chem. 2014, 79, 559−570

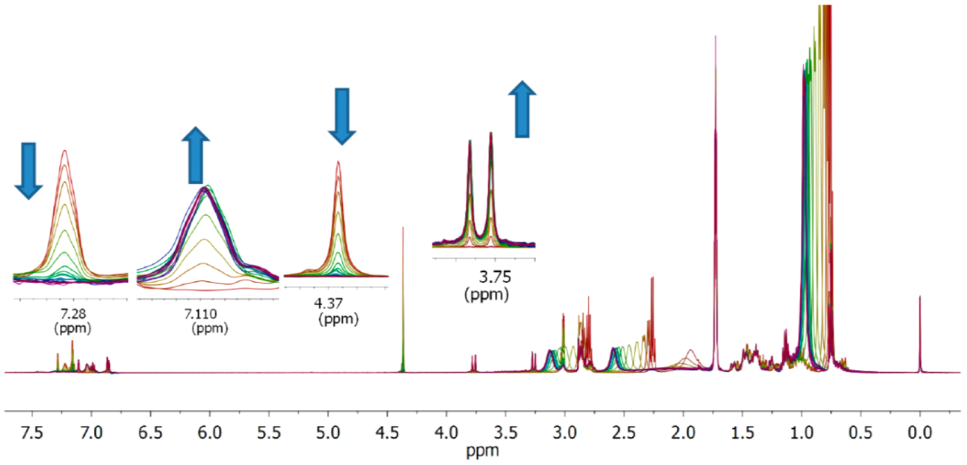

Figure 11. Overlapped ^{1}H NMR spectra for the kinetic experiment leading to the formation of macrocycle **2f**.

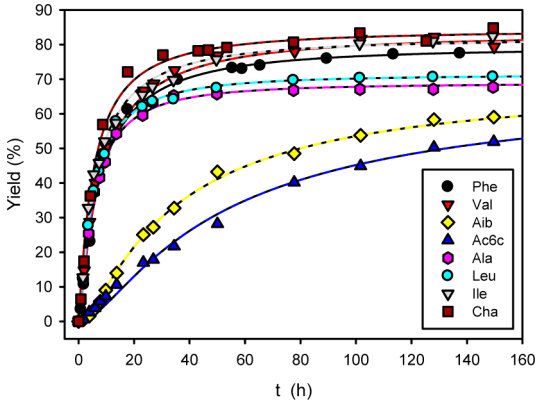

Figure 12. Kinetic curves obtained from ^{1}H NMR experiments for the formation of the different macrocycles **2** (7.5 mM) under the same reaction conditions (0.5 equiv of bromide anion, deuterated acetonitrile, 25 °C, 10 equiv of DIPEA as the base). For clarity, only the data for the first 160 h of reaction have been displayed.

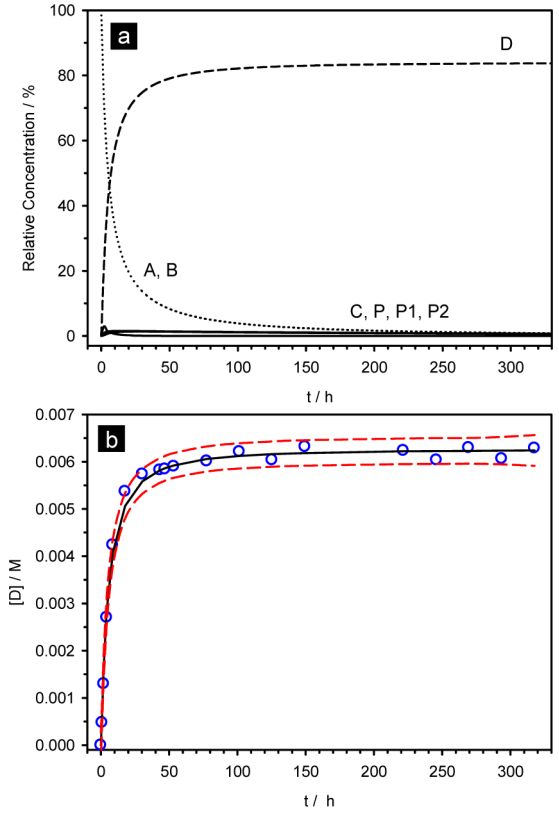

Figure 13. (a) Time variation of the concentrations of the different species modeled according to the simplified kinetic model for **2f**. Dotted lines: curve A, **1f**; curve B, 1,3-bis(bromomethyl)benzene. Dashed line: curve C, reaction intermediate **3f**. Solid line: curve D, macrocyclic product **2f**. Complete overlap of the curves corresponding to the starting materials is observed. (b) Time variation of the concentration of macrocyclic compound **2f** using the optimized conditions. The black solid curve was obtained from the calculated k_1 and k_2 values, and the red dashed lines represent the standard deviations. Blue open circles show the experimental data.

according to this kinetic model using the calculated kinetic parameters [curve A, **1f**; curve B, 1,3-bis(bromomethyl)-benzene; curve C, **3f**; curve D, **2f**]. Complete overlap of the experimental and calculated curves corresponding to the starting materials was observed (Figure 13b). It can be seen that the concentrations of the intermediate and the oligomers are very low for the whole time span.

Table 1 summarizes the kinetic constants obtained from the corresponding fits using the Mathematica software and the developed kinetic model.[37] The associated errors have been included for all cases. Moreover, the Eyring equation, $k = (k_B T/h)\exp(-\Delta G^{\ddagger}/RT)$,[38,39] was employed to calculate the Gibbs free energy barrier between the reactant interaction complex and the transition state. The kinetic constants k_1 associated with the first reaction step for the tertiary amino acids Ala, Cha, and Leu are ca. 25 M^{-1} h^{-1}, indicating that the substitution of one H atom in the β-carbon has a minor influence on the this kinetic constant. Interestingly, Phe, which contains a phenyl ring that favors the formation of aggregates and should decrease its reactivity, shows a smaller k_1 of 18 M^{-1} h^{-1}.[40,41] The substitution of two H atoms on the β-carbon has a small but perceptible influence on the kinetic constant of the first reaction step. Thus, Val and Ile have k_1 = 17 and 21 M^{-1} h^{-1}, respectively. In sharp contrast, an additional substitution at the α-carbon atom has a dramatic influence on k_1, and the k_1 values for the quaternary amino acids are consistently lower by factors of 7−10. Similar k_1 values were obtained for the two quaternary amino acids, indicating again that substitution at the β-carbon has a minor influence. A decrease of 34% in k_1, similar to that observed in going from Ala to Val (33%), was observed.

dx.doi.org/10.1021/jo4022309 | J. Org. Chem. 2014, 79, 559−570

Table 1. Kinetic Parameters Obtained for the Different Cyclization Reactions from Open-Chain Pseudopeptides 1[a]

1	Aaa	k_1 (M^{-1} h^{-1})	k_2 (h^{-1})	$\Delta G_1^{\ddagger}$ (kcal mol^{-1})	$\Delta G_2^{\ddagger}$ (kcal mol^{-1})	$\Delta\Delta G^{\ddagger}$ (kcal mol^{-1})[b]
1a	Phe	17.54 ± 0.01	1.53 ± 0.14	20.60 ± 0.01	22.05 ± 0.05	1.45 ± 0.06
1b	Val	16.5 ± 1.3	1.94 ± 0.20	20.64 ± 0.05	21.91 ± 0.06	1.27 ± 0.11
1c	Ala	24.8 ± 1.0	1.145 ± 0.001	20.40 ± 0.02	22.22 ± 0.01	1.82 ± 0.03
1d	Aib	3.65 ± 0.11	0.158 ± 0.004	21.54 ± 0.02	23.40 ± 0.01	1.86 ± 0.03
1e	Ac6c	2.40 ± 0.12	0.094 ± 0.003	21.78 ± 0.03	23.70 ± 0.02	1.92 ± 0.05
1f	Cha	24.9 ± 2.5	3.211 ± 0.001	20.40 ± 0.06	21.61 ± 0.01	1.21 ± 0.07
1g	Ile	21.42 ± 1.5	2.29 ± 0.20	20.49 ± 0.05	21.81 ± 0.05	1.32 ± 0.10
1h	Leu	25.0 ± 1.0	1.33 ± 0.04	20.40 ± 0.02	22.13 ± 0.02	1.73 ± 0.04

[a]Compound **1i** (Aaa = Gly) was found to yield only oligomers; the macrocycle could not be isolated from the reaction mixture.[42] This compound has low solubility under the reaction conditions. [b]$\Delta\Delta G^{\ddagger} = \Delta G_2^{\ddagger} - \Delta G_1^{\ddagger}$.

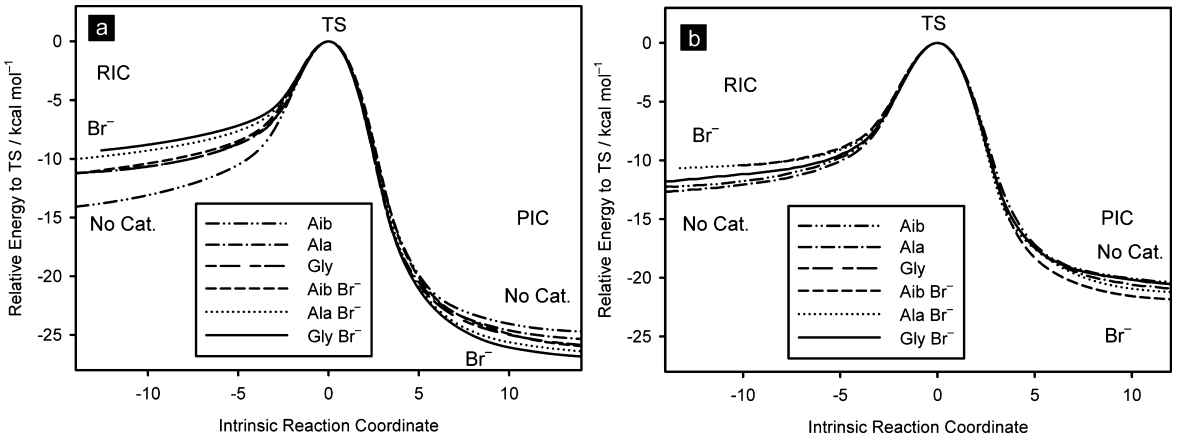

Figure 14. IRC profiles for the macrocyclization reaction steps of pseudopeptides **1** with 1,3-bis(bromomethyl)benzene in acetonitrile in the absence or presence of bromide computed at the B3LYP/6-31G* level of theory: (a) first reaction step; (b) second reaction step.

However, the values of the kinetic constant k_2 associated with the macrocyclization step for the quaternary amino acids (0.10−0.15 h^{-1}) are 8−30 times lower than those for the tertiary amino acids (3.2−1.2 h^{-1}). This provides evidence that the substituent has a more pronounced effect on the macrocyclization step. Interestingly, this effect is not directly related to the volume of the substituent.

For this system (Figure 1), the yield obtained in the macrocyclization reaction must be related to the k_2/k_1 ratio. As the first step is common for oligomerization and cyclization, this ratio determines the relative rates at which macrocycles and oligomers are formed. Consequently, the simplest way to analyze our results is through the corresponding values of $\Delta\Delta G^{\ddagger} = \Delta G_2^{\ddagger} - \Delta G_1^{\ddagger}$ gathered in Table 1. The yields are higher for systems displaying smaller values of $\Delta\Delta G^{\ddagger}$.

It can be seen that the cyclohexylalanine derivative (**1f**) has the lowest difference between the energy barriers for the macrocyclization and the first reaction. On the contrary, the compounds derived from quaternary amino acids (**1d** and **1e**) are the least favorable for macrocyclization and also present the highest energy barriers for both reaction steps. Although large variations were observed among the other compounds, no clear structural trends could be detected. Thus, the less hindered Ala derivative (**1c**) is less favorable for cyclization than the sterically more demanding Val derivative (**1b**) ($\Delta\Delta G^{\ddagger}$ = 1.82 and 1.27 kcal mol^{-1}, respectively). This is essentially associated with the difference in the energy barriers for the cyclization step, for which the conformational effects are critical, suggesting a complex effect of the side chains beyond their steric volume. As can be seen, except for the quaternary amino acid derivatives, differences in the energy barrier for k_1 are very small (<0.25 kcal mol^{-1}) while the differences for the second step are more significant (up to 0.60 kcal mol^{-1}).

The data from the kinetic studies were also useful for determining the reaction parameters for the syntheses of the different macrocycles on a synthetic scale.[22,43] In all cases, the yields obtained were in excellent agreement with the results from the kinetic analysis. However, for the quaternary amino acid derivatives, the formation of larger amounts of side products led to more difficult purification processes, significantly decreasing the final isolated yields.

Ab Initio Calculations. No direct correlations could be found between the experimental data and the parameters obtained by molecular mechanics calculations (i.e., the average C···N distance for the reaction intermediate **3**). Accordingly, an in silico study of these processes was carried out by means of reaction profile calculations. A kinetic analysis involves calculating the transition state that connects reactants and products and the energy barrier between them.[24] For this purpose, we selected the systems derived from the amino acids Aib, Ala, and Gly. Their sizes still allow the use of high-level calculations. On the other hand, they represent a well-defined family of derivatives for which the substitution at the α-carbon increases steadily.

Both reaction steps were modeled with the presence of added bromide anion as a catalytic species taken into account. The structures of the reactants, complexes of interaction of reactants (RICs), transition states (TSs), complexes of interaction of products (PICs), and products were optimized to obtain the corresponding reaction profiles.[43,44]

An initial potential energy surface (PES) calculation at the PM3 level of theory allowed the approximate TS geometry as

dx.doi.org/10.1021/jo4022309 | J. Org. Chem. 2014, 79, 559−570

well as those for the other stationary points to be found (see Figures S-3 and S-4 in the Supporting Information for the transformation of **1c**). These structures were then fully optimized at the B3LYP/6-31G* level of theory in the presence of solvent (acetonitrile) using the self-consistent reaction field (SCRF) theory, which performs polarized continuum model (PCM) calculations.[45−47] From these optimized TSs, intrinsic reaction coordinate (IRC) calculations were completed in order to obtain the whole reaction profile.[48] The last geometries at both ends of the IRC path were optimized in order to obtain the corresponding optimized geometries of the completely true RIC and PIC minima (Figure 14).

The optimized geometries of the transition states for **1c, 1d,** and **1i** for the first and second reaction steps in the absence of anion are represented in Figures 15a,c,e and 16a,c,e,

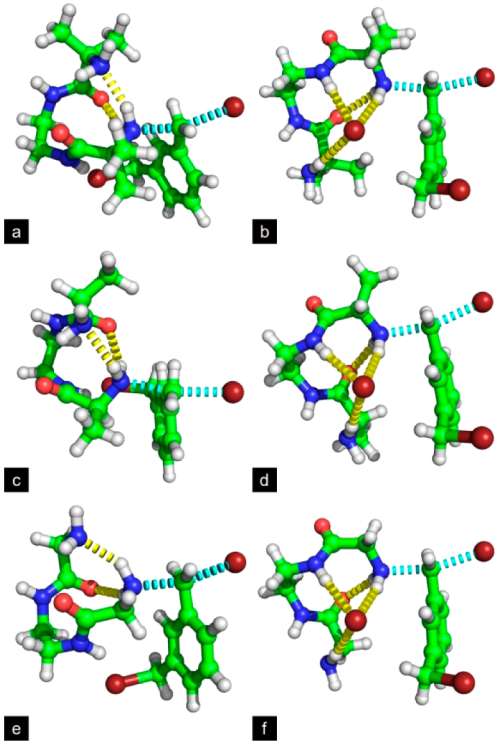

Figure 15. TSs for the first step of the reaction of **1** with 1,3-bis(bromomethyl)benzene in acetonitrile in (a, c, e) the absence and (b, d, f) the presence of bromide, calculated at the B3LYP/6-31G* level of theory: (a) **1d** Aib; (b) **1d** Aib + Br^-; (c) **1c** Ala; (d) **1c** Ala + Br^-; (e) **1i** Gly; (f) **1i** Gly + Br^-.

respectively. In all cases, an intramolecular H-bond between the oxygen atom of a carbonyl group and one hydrogen atom of the reactive amine is observed. This preorganizes the reaction intermediate and helps to reduce the positive partial charge evolving on the amine group during its transformation into an ammonium group. Moreover, for the geometries for the first reaction step, the higher flexibility of the open-chain compounds allows for an additional H-bond between the N atom of the nonreacting amine and the second hydrogen atom of the reacting amine, which also stabilizes the developing ammonium group. In the case of the macrocyclization step, this second stabilizing H-bond is not possible.

In contrast, in the presence of bromide (Figures 15b,d,e and 16b,d,e) the intramolecular H-bond between the oxygen atom of the carbonyl group and one of the hydrogen atoms of the

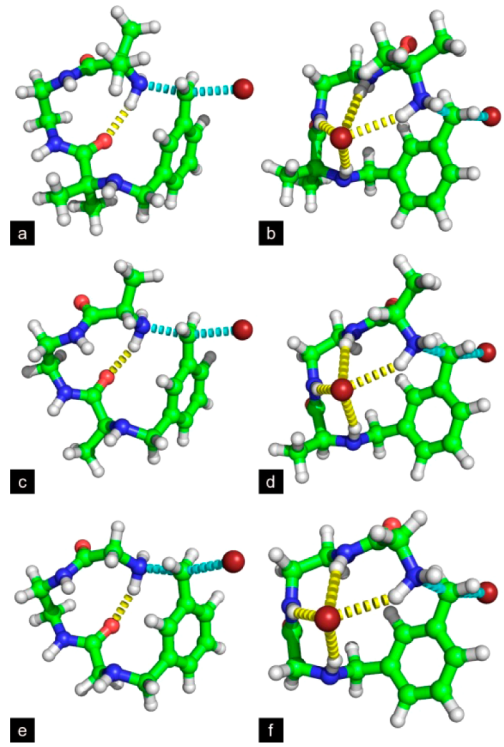

Figure 16. TSs for the macrocyclization step of the reaction of **1** with 1,3-bis(bromomethyl)benzene in acetonitrile in (a, c, e) the absence and (b, d, f) the presence of bromide, calculated B3LYP/6-31G* level of theory: (a) **1d** Aib; (b) **1d** Aib + Br^-; (c) **1c** Ala; (d) **1c** Ala + Br^-; (e) **1i** Gly; (f) **1i** Gly + Br^-.

reactive amine is observed only for the first step, but the anion forms additional H-bonds with the different amine and amide groups. In the first reaction step, *three* H-bonds between the bromide and the hydrogen atoms of one amide and the two amines are observed. In the macrocyclization step, however, *four* H-bonds are observed with the bromide, involving the two amide hydrogen atoms and one hydrogen atom of each amino group. This preorganizes the system and neutralizes the increment on the partial charge on the amine group as it becomes an ammonium group as the reaction advances. The overall result is a decrease in the energy barrier between the reactants and products.

In order to analyze the influence of the side chain of the constituent amino acid and to compare the computational data with the kinetic results previously obtained, the RIC−TS Gibbs free energy barriers, entropy changes, and enthalpy barriers were calculated. Table 2 summarizes the results obtained for

Table 2. RIC−TS Gibbs Free Energy Barriers (kcal mol^{-1}) for Both Reaction Steps

	Aaa	no catalyst	Br^- catalyst
ΔG_{RIC-TS} for first reaction step	Aib	19.66	17.64
	Ala	15.38	15.26
	Gly	15.08	14.68
ΔG_{RIC-TS} for macrocyclization step	Aib	19.41	15.22
	Ala	17.25	15.12
	Gly	17.19	15.13
$\Delta\Delta G_{RIC-TS}$	Aib	−0.25	−2.42
	Ala	1.87	−0.14
	Gly	2.11	0.45

dx.doi.org/10.1021/jo4022309 | J. Org. Chem. 2014, 79, 559−570

both reaction steps for **1d** (Aib), **1c** (Ala), and **1i** (Gly). It can be observed that the anion significantly reduces the calculated ΔG_{RIC-TS} energy barriers in acetonitrile. The corresponding calculated entropy and enthalpy barriers (see Tables S1−S3 in the Supporting Information) are presented in Figure 17.

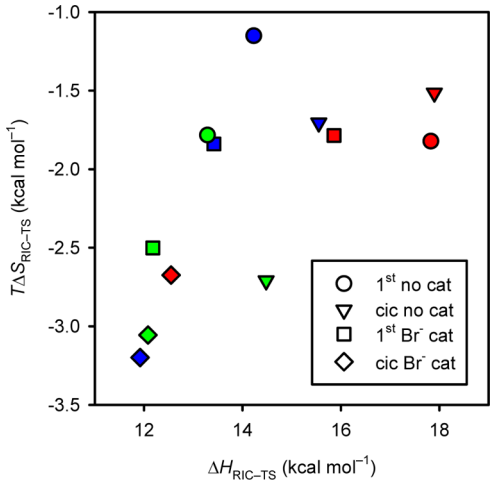

Figure 17. Enthalpy vs entropy plots (T = 298.15 K) for both reaction steps in acetonitrile, calculated at the B3LYP/6-31G* level of theory: Aib, red; Ala, blue; Gly, green.

The calculated entropy change for going from the RIC to the TS is negative in all cases, as expected in an S_N2 reaction. From the ΔS_{RIC-TS} values it must be pointed out that in the case of the Br^--catalyzed reaction in acetonitrile, the value of ΔS_{RIC-TS} for the macrocyclization step is more negative than that for first reaction step. Therefore, the use of low temperatures will favor the formation of the macrocycle as long as the negative contribution of the enthalpy to the RIC−TS free energy barrier will be reduced. Regarding the enthalpy change from RIC to TS, the lowest ΔH_{RIC-TS} value was obtained for the macrocyclization step catalyzed by bromide in acetonitrile (diamonds in Figure 17), in good agreement with our initial selection of working hypotheses.

The values show that the energy barrier for the first reaction step increases significantly with the steric hindrance of the amino acid side chain in the absence and presence of Br^-. The same trend is observed for the second step in the absence of bromide. On the contrary, the calculations suggest that the amino acid side chain has essentially no effect on the macrocyclization energy barrier in the presence of the anion. Thus, the data in Table 2 explain the catalytic effect observed experimentally for the presence of the bromide anion but do not allow a simple explanation of the effects detected for the changes in the side chain.

In this regard, the existence of different conformers for each open-chain intermediate and their populations at equilibrium needs to be considered. According to the data obtained from the MMFF calculations, the structures of such conformers and their relative energies are strongly dependent on the nature of the side chain. In such equilibria, we can consider that a reactive conformation must have the appropriate geometry (RIC) to react to afford the products. Thus, the low-energy conformers obtained from the Monte Carlo conformational searches at the MMFF level of theory were optimized at the B3LYP/6-31G* level of theory in acetonitrile. The relative energies of the RIC relative to that of the most stable conformer are shown in Table 3, and the corresponding Boltzmann distributions of the RIC (% abundance) are shown in Table 4. The amino acid side chain has a direct influence on the Boltzmann distribution, although a simple correlation with the size does not exist, particularly in the presence of Br^-. In all cases, the RIC is less stable than the most stable conformer, but this unfavorable energy difference is much less important in the presence of Br^-. Therefore, the effect of the anion is double: it reduces the RIC−TS energy barrier and increases the population of reactive RIC molecules.

Table 3. Relative Gibbs Free Energies of the RIC Relative to the Most Stable Calculated Conformer for Both Reaction Steps at 25 °C (B3LYP/6-31G*, Acetonitrile)

		ΔG (kcal mol^{-1})	
reaction step	Aaa	no catalyst	Br^- catalyst
first step	Aib	8.21	0.466
	Ala	6.03	0.446
	Gly	5.48	1.58
macrocyclization step	Aib	9.89	1.92
	Ala	8.01	1.26
	Gly	7.17	1.79

Table 4. Boltzmann Distributions of the RIC (%) for Both Reaction Steps at 25 °C (B3LYP/6-31G*, Acetonitrile)

		Boltzmann population (%)	
reaction step	Aaa	no catalyst	Br^- catalyst
first step	Aib	0.00829	19.06
	Ala	0.0731	19.43
	Gly	0.1264	6.25
macrocyclization step	Aib	0.00154	4.45
	Ala	0.0101	8.64
	Gly	0.0233	5.06

Thus, in the presence of the catalytic anion, the amino acid side chain has an effect on both the conformation and the ΔG_{RIC-TS} barrier for the first reaction step, while for the critical macrocyclization step the changes in the side chain are reflected only in changes in the conformational equilibria of the open-chain precursor. This highlights the importance of the amino acid side chain on the preorganization of the open-chain precursor with the appropriate folded conformation (RIC). These results are in nice agreement with our previous studies with 2,6-bis(aminomethyl)pyridine, in which the side chain of the constituent amino acid had a minor role as long as the pyridine spacer itself facilitated the folding of the open-chain precursor to a proper conformation.[24] As could be expected, other factors associated with the side chain besides the steric volume, such as the hydrophobic/hydrophilic character or the possibility of participating in supramolecular interactions, can be of importance for determining the corresponding conformational equilibria of the open-chain intermediates **3**.

Taking into account both the calculated energy barriers and the Boltzman partition function of the RIC, the corresponding reaction kinetics for the formation of the macrocyclic compound can be predicted, as shown in Figure 18.[24,37] As can be seen, there is an excellent match between the trends detected by the calculations and the ones observed experimentally (Figure 12).

dx.doi.org/10.1021/jo4022309 | J. Org. Chem. 2014, 79, 559−570

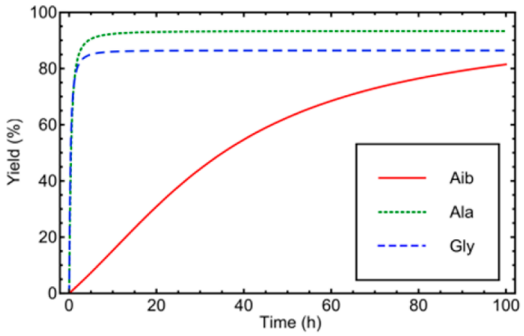

Figure 18. Simulation of the macrocyclization reaction kinetics from the B3LYP/6-31G*-calculated energy barriers in acetonitrile. $[\mathbf{1}]_0$ = $[1,3\text{-bis(bromomethyl)benzene}]_0$ = 7.450 mM and $[Br^-]_0$ = 3.725 mM at 25 °C in acetonitrile.

CONCLUSIONS

Both experimental results and theoretical calculations show that the amino acid side chain plays a critical role in the preorganization of pseudopeptides and therefore in their macrocyclization tendency. An increase in the number of substituents on the α carbon atom (quaternary amino acids) decreases the macrocyclization reaction rate significantly. The overall observed effect for the change in the side chain of the constituent amino acid is not directly related to its size but rather involves the modification of the conformational preferences of the open-chain intermediate **3**.

Among the different compounds studied, compound **1d** derived from cyclohexylalanine is the one that cyclizes more efficiently. The calculations revealed that in this case the most stable conformation in the presence of the bromide anion approximates very efficiently, with the correct orientation, the two reactive ends of the reaction intermediate. Thus, the selection of the appropriate amino acid can play a key role in determining the success of a macrocyclization in peptidic or pseudopeptidic structures.

The excellent agreement between the experimental and computational results highlights the potential of the appropriate use of computational modeling of open-chain intermediates to predict their tendencies to cyclize. For this purpose, the corresponding energy barriers are not the only parameters to be considered, and the associated conformational equilibria of the open-chain intermediates have to be considered in detail. Therefore, this methodology can be efficiently used in the design of new macrocyclic peptidic and pseudopeptidic structures and the most appropriate synthetic routes for their preparation.

EXPERIMENTAL SECTION

The NMR experiments were carried out at 500 or 300 MHz for ^{1}H and 125 or 75 MHz for ^{13}C. Chemical shifts are reported in parts per million from tetramethylsilane with the solvent resonance as the internal standard. FT-IR spectra were recorded using an instrument with a MIRacle Single Reflection ATR Diamond/ZnSe accessory. Microanalyses were performed on an elemental analyzer. Mass spectra were recorded with a Q-TOF instrument. Rotatory power was determined with a digital polarimeter (Na: 589 nm). Melting points were measured using a standard apparatus and are uncorrected.

ESI-MS Experiments. The crude reaction product in acetonitrile, which contained some precipitates because of the poor solubility of the oligomers in acetonitrile, was solubilized in a DMSO/methanol 1:1 (v/v) mixture and diluted to the appropriate concentration for the mass spectrometer. The samples were measured in the ESI-MS apparatus in positive mode at 20 and 45 V to improve the resolution of high-mass polymers.

NMR Kinetic Experiments. The macrocyclization reactions were followed by ^{1}H NMR spectroscopy. Tetrakis(trimethylsilyl)silane was used as an internal standard to reference the peaks and the integrals of the different signals of the reactants and products. This allowed the quantification of the signals of the product of the macrocyclization reaction and those corresponding to the starting reactants. It was checked in an isothermal experiment at 25 °C, using a constant gain of the NMR receiver, that the integral of the internal standard was not disturbed under the reaction conditions. The different experiments were performed directly in NMR tubes at 25 °C with 1.00 mL of deuterated acetonitrile. In this way the macrocyclization reaction could be monitored using very small amounts of reactants.

All of the reactants, bis(amino amide) (1.723 mg, 0.00747 mmol for compound **1d**), TBABr (1.206 mg, 0.00374 mmol), DIPEA (12.81 μL, 0.07482 mmol), and internal standard tetrakis(trimethylsilyl)silane (0.1333 mg, 0.004156 mmol), were placed in a vial, and then deuterated acetonitrile (1.00 mL) was added. The reaction mixture was stirred and heated until a clear solution was obtained. Then 1,3-bis(bromomethyl)benzene was weighed in a second vial (1.974 mg, 0.00747 mmol). The reaction mixture was transferred quantitatively to the NMR tube; this was inserted into the NMR probe and allowed to equilibrate. Then the lock and shim were adjusted, and a reference ^{1}H NMR was acquired. After that, the contents of the NMR tube were quantitatively poured into the vial containing 1,3-bis(bromomethyl)-benzene and immediately put back to the NMR tube. The lock and shim were adjusted again. The ^{1}H NMR spectra were acquired at different times until the end of the reaction.

Computational Details. All of the structures were minimized using Gaussian 09.[49] Calculations were performed in acetonitrile using the SCRF methodology. The true nature of the minima was demonstrated by a normal mode of vibration analysis. For TSs, one single negative eigenvalue was found, corresponding to the reaction path involving the breaking and forming bonds. For the other structures, all of the eigenvalues were positive. Monte Carlo conformational searches using the MMFF force field were carried out with the Spartan'08 software.[50]

Synthesis of Compounds. Bis(amino amine)s **1a**, **1b**, **1c**, **1g**, **1h**, and **1i** and macrocycles **2a**, **2b**, **2c**, **2g**, and **2h** were prepared using the conditions previously reported.[22,43]

*General Procedure for the Synthesis of Boc-Protected Bis(amino amide)s: Synthesis of tert-Butyl N-(1-{[2-(2-{[(tert-Butoxy)carbonyl]-amino}-2-methylpropanamido)ethyl]carbamoyl}-1-methylethyl)-carbamate (**1d-Boc**).* Boc-Aib-OH (1.455 g, 7.160 mmol) was placed in a 250 mL round-bottom flask, and dry acetonitrile (100 mL) was added. BOP (2.802 g, 8.596 mmol) was then added to the reaction mixture, followed by DIPEA (1.497 mL, 8.596 mmol). The reaction was stirred for 30 min at rt under a nitrogen atmosphere, and then ethylenediamine (239 μL, 3.580 mmol) was added. The reaction was kept for 1 day at rt, and then the solvent was eliminated under reduced pressure. The obtained oil was dissolved in dichloromethane (50 mL) and washed with a 5% solution of $KHSO_4$ (3 × 20 mL), a 5% solution of $NaHCO_3$ (3 × 20 mL), and water (3 × 20 mL). The organic layer was dried with $MgSO_4$, and the solvent was evaporated under reduced pressure to obtain a white foam. The product was purified by column chromatography on flash silica gel [3 cm diameter, 15 cm height; mobile phases: CH_2Cl_2/MeOH 20:1 to 10:1 v/v (mL/mL)]. The pure product was collected in fractions 3−5 as a white solid (2.682 g, 6.229 mmol, 87% yield). Mp 234−235 °C; IR (ATR) 3330, 2979, 2930, 1688, 1659, 1545, 1518, 1449, 1388, 1364 cm^{-1}; ^{1}H NMR (500 MHz, DMSO-d_6) δ 1.25 (6H, s), 1.34 (9H, s), 3.05 (2H, s), 6.79 (1H, s), 7.51 (1H, s); ^{13}C NMR (126 MHz, DMSO-d_6) δ 25.6, 28.6, 39.3, 56.0, 78.3, 154.6, 174.9; HRMS (ESI-TOF)$^+$ calcd for $C_{20}H_{38}N_4O_6$ (M + Na)$^+$ 453.2689, found 453.2685. Anal. Calcd for $C_{20}H_{38}N_4O_6$: C, 55.79; H, 8.90; N, 13.01. Found: C, 55.44; H, 8.68; N, 12.89.

*Synthesis of tert-Butyl N-[1-({2-[(1-{[(tert-Butoxy)carbonyl]-amino}cyclohexyl)formamido]ethyl}carbamoyl)cyclohexyl]-carbamate (**1e-Boc**).* This compound was prepared using the general procedure described above as a white solid (1.350 g, 2.64 mmol, 26%

dx.doi.org/10.1021/jo4022309 | J. Org. Chem. 2014, 79, 559−570

yield). Mp 179−180 °C; IR (ATR) 3320, 2980, 2934, 2852, 1686, 1644, 1542, 1515, 1453, 1390, 1365 cm^{-1}; ^1H NMR (500 MHz, DMSO-d_6) δ 1.11−1.19 (2H, m), 1.35 (18H, s), 1.36−1.51 (12H, m), 1.52−1.65 (4H, m), 1.67−1.96 (4H, m), 3.04 (4H, s), 6.54 (2H, s), 7.39 (2H, s); ^{13}C NMR (126 MHz, DMSO-d_6) δ 21.1, 25.1, 28.2, 31.8, 38.8, 58.4, 77.9, 154.3, 174.7; HRMS (ESI-TOF)$^+$ calcd for $C_{26}H_{46}N_4O_6$ (M + Na)$^+$ 533.3315, found 533.3321. Anal. Calcd for $C_{26}H_{46}N_4O_6$: C, 61.15; H, 9.08; N, 10.97. Found: C, 60.77; H, 9.04; N, 10.90.

*Synthesis of tert-Butyl N-[(1S)-1-({2-[(2S)-2-{[(tert-Butoxy)-carbonyl]amino}-3-cyclohexylpropanamido]ethyl}carbamoyl)-2-cyclohexylethyl]carbamate (**1f-Boc**).* This compound was prepared using the general procedure described above as a white solid (1.732 g, 3.056 mmol, 44% yield). Mp 170−171 °C; $[\alpha]_D^{25}$ = +56.40 (c = 0.01, $CHCl_3$); IR (ATR) 3340, 2923, 2852, 1680, 1661, 1520, 1446, 1392, 1368 cm^{-1}; ^1H NMR (500 MHz, DMSO-d_6) δ 0.75−0.90 (4H, m), 1.03−1.17 (6H, m), 1.19−1.26 (2H, m), 1.32−1.39 (22H, m), 1.53−1.65 (8H, m), 1.71 (2H, d, J = 12.6 Hz), 2.95−3.15 (4H, m), 3.90 (2H, dd, J = 8.7, 14.6 Hz), 6.73 (2H, d, J = 8.2 Hz), 7.77 (2H, s); ^{13}C NMR (75 MHz, DMSO-d_6) δ 26.1, 26.3, 26.5, 28.6, 32.3, 33.7, 34.1, 38.8, 52.5, 78.4, 155.8, 173.2; HRMS (ESI-TOF)$^+$ calcd for $C_{30}H_{54}N_4O_6$ (M + Na)$^+$ 589.3941, found 589.3940. Anal. Calcd for $C_{30}H_{54}N_4O_6$: C, 63.57; H, 9.60; N, 9.89. Found: C, 63.29; H, 9.31; N, 10.12.

*General Procedure for the Deprotection of Boc-Protected Bis(amino amide)s: Synthesis of 2-Amino-N-[2-(2-amino-2-methylpropanamido)ethyl]-2-methylpropanamide (**1d**).* Compound **1d-Boc** (679 mg, 1.577 mmol) was dissolved in the minimum quantity of dichloromethane (80 mL) by reflux heating, and then TFA (10 mL) was added. The reaction was stirred under a nitrogen atmosphere for 1 h, and then the solvent was removed under vacuum. Water (10 mL) was added, and the mixture was basicified to pH 12 with solid NaOH and extracted with $CHCl_3$ (3 × 25 mL). The organic layers were combined and dried with anhydrous $MgSO_4$. The solvent was evaporated under reduced pressure. The product was obtained as a white solid (241 mg, 1.046 mmol, 66% yield). Mp 114−115 °C; IR (ATR) 3384, 3283, 2972, 2934, 1630, 1519, 1442, 1375, 1357 cm^{-1}; ^1H NMR (500 MHz, $CDCl_3$) δ 1.32 (6H, s), 1.42 (2H, s), 3.35 (2H, dd, J = 2.5, 3.1 Hz), 7.90 (1H, s); ^{13}C NMR (126 MHz, $CDCl_3$) δ 29.2, 39.6, 54.7, 178.5; HRMS (ESI-TOF)$^+$ calcd for $C_{10}H_{22}N_4O_2$ (M + H)$^+$ 231.1821, found 231.1815. Anal. Calcd for $C_{10}H_{22}N_4O_2$: C, 52.15; H, 9.63; N, 24.33. Found: C, 52.04; H, 9.26; N, 23.99.

*Synthesis of 1-Amino-N-{2-[(1-aminocyclohexyl)formamido]-ethyl}cyclohexane-1-carboxamide (**1e**).* This compound was prepared using the general procedure described above as a white solid (410 mg, 1.321 mmol, 72% yield). Mp 149−150 °C; IR (ATR) 3338, 3284, 2921, 2851, 1649, 1598, 1444, 1361 cm^{-1}; ^1H NMR (500 MHz, $CDCl_3$) δ 1.21−1.34 (6H, m), 1.35−1.44 (8H, m), 1.56−1.63 (6H, m), 1.88−1.97 (4H, m), 3.30−3.35 (4H, m), 8.05 (2H, s); ^{13}C NMR (126 MHz, $CDCl_3$) δ 21.3, 25.3, 34.7, 39.6, 57.3, 178.9; HRMS (ESI-TOF)$^+$ calcd for $C_{16}H_{30}N_4O_2$ (M + H)$^+$ 311.2447, found 311.2438. Anal. Calcd for $C_{16}H_{30}N_4O_2$: C, 61.90; H, 9.74; N, 18.05. Found: C, 61.58; H, 9.56; N, 17.86.

*Synthesis of (2S)-2-Amino-N-{2-[(2S)-2-amino-3-cyclohexyl-propanamido]ethyl}3-cycloexylropanamide (**1f**).* This compound was prepared using the general procedure described above as a white solid (837 mg, 1.477 mmol, 55% yield). Mp 131−132 °C; $[\alpha]_D^{25}$ = −31.34 (c = 0.01, $CHCl_3$); IR (ATR) 3330, 3301, 2979, 2930, 1688, 1659, 1546, 1518, 1449, 1388, 1364 cm^{-1}; ^1H NMR (500 MHz, $CDCl_3$) δ 0.84−1.01 (4H, m), 1.09−1.30 (8H, m), 1.33−1.46 (6H, m), 1.59−1.78 (12H, m), 3.37 (6H, s), 7.64 (2H, s); ^{13}C NMR (126 MHz, $CDCl_3$) δ 26.2, 26.5, 26.6, 32.2, 34.3, 34.4, 39.6, 42.9, 52.9, 176.9; HRMS (ESI-TOF)$^+$ calcd for $C_{20}H_{38}N_4O_2$ (M + H)$^+$ 367.3073, found 367.3066. Anal. Calcd for $C_{20}H_{38}N_4O_2$: C, 65.54; H, 10.45; N, 15.29. Found: C, 65.40; H, 10.06; N, 15.15.

*General Procedure for the Macrocyclization of Bis(amino amide)s: Synthesis of 4,4,11,11-Tetramethyl-3,6,9,12-tetraazabicyclo[12.3.1]octadeca-1(18),14,16-triene-5,10-dione (**2d**).* Compound **1d** (100 mg, 0.434 mmol), TBABr (70.0 mg, 0.217 mmol), and DIPEA (743 mL, 4.343 mmol) were placed in a 250 mL round-bottom flask, and then dry acetonitrile (120 mL) was added. The reaction mixture was heated until all of the reactants were dissolved. Then 1,3-bis(bromomethyl)benzene (114.6 mg, 0.434 mmol) was weighed and dissolved into a small quantity of dry acetonitrile and placed into the reaction flask. The reaction mixture was stirred for 3 weeks at 25 °C under a nitrogen atmosphere. The solvent was removed under reduced pressure to obtain the crude reaction as a foam. The foam was dissolved in $CHCl_3$ (25 mL) and washed with water (3 × 25 mL). The organic layer was dried with anhydrous magnesium sulfate and evaporated to dryness. Purification of this product was carried out by column chromatography with flash silica gel (50 g). CH_2Cl_2/MeOH mixtures (from 10:0 to 10:2 v/v) containing a few drops of aqueous ammonia to prevent the retention of amines in the column were used as the mobile phase. Macrocycle **2d** was obtained as a white solid (15 mg, 0.045 mmol, 10% yield). Mp 187−188 °C; IR (ATR) 3357, 3301, 2981, 2945, 1645, 1506, 1480, 1441, 1378, 1361 cm^{-1}; ^1H NMR (500 MHz, $CDCl_3$) δ 1.38 (12H, s), 1.61 (2H, s), 3.37 (4H, s), 3.72 (4H, s), 7.08 (2H, d, J = 6.7 Hz), 7.22−7.26 (1H, m), 7.57 (1H, s), 7.92 (2H, s); ^{13}C NMR (75 MHz, $CDCl_3$) δ 25.9, 39.7, 48.3, 59.4, 126.4, 128.7, 129.0, 141.6, 177.5; HRMS (ESI-TOF)$^+$ calcd for $C_{18}H_{28}N_4O_2$ (M + H)$^+$ 333.2291, found 333.2294. Anal. Calcd for $C_{18}H_{28}N_4O_2$: C, 65.03; H, 8.49; N, 16.85. Found: C, 64.72; H, 8.62; N, 16.57.

*Synthesis of Dispiro[cyclohexane-1,4′-[3,6,9,12]tetraazabicyclo-[12.3.1]octadecane-11′,1″-cyclohexane]-1′(17′),14′(18′),15′-triene-5′,10′-dione (**2e**).* This compound was prepared using the general procedure described above. The macrocycle was obtained as a white solid (18 mg, 0.0436 mmol, 9% yield). Mp 192−193 °C; IR (ATR) 3319, 2918, 2856, 1662, 1498, 1479, 1458, 1445, 1427, 1354 cm^{-1}; ^1H NMR (500 MHz, $CDCl_3$) δ 1.06−1.25 (19H, m), 1.41−1.55 (31H, m), 1.64−1.74 (19H, m), 3.17 (12H, s), 3.42 (12H, s), 6.92 (6H, d, J = 7.4 Hz), 7.06−7.11 (3H, m), 7.33 (3H, s), 7.66 (6H, s); ^{13}C NMR (75 MHz, $CDCl_3$) δ 21.7, 25.1, 32.1, 40.0, 47.7, 61.9, 126.7, 128.8, 129.9, 141.7, 177.8; HRMS (ESI-TOF)$^+$ calcd for $C_{24}H_{36}N_4O_2$ (M + H)$^+$ 413.2917, found 413.2913. Anal. Calcd for $C_{24}H_{36}N_4O_2$: C, 69.87; H, 8.80; N, 13.58. Found: C, 69.59; H, 8.88; N, 13.63.

*Synthesis of (4S,11S)-4,11-Bis(cyclohexylmethyl)-3,6,9,12-tetraazabicyclo[12.3.1]octadeca-1(18),14,16-triene-5,10-dione (**2f**).* This compound was prepared using the general procedure described above. The macrocycle was obtained as a white solid (114 mg, 0.2432 mmol, 45% yield). Mp 199−200 °C; $[\alpha]_D^{25}$ = +8.75 (c = 0.01, $CHCl_3$); IR (ATR) 3344, 3306, 2921, 2846, 1654, 1520, 1447, 1362, 1323 cm^{-1}; ^1H NMR (500 MHz, $CDCl_3$) δ 0.89−1.02 (4H, m), 1.10−1.30 (6H, m), 1.31−1.46 (4H, m), 1.62−1.82 (12H, m), 1.83 (2H, s), 2.99−3.08 (4H, m), 3.21 (2H, dd, J = 4.3, 9.3 Hz), 3.52 (2H, d, J = 13.1 Hz), 4.05 (2H, d, J = 13.1 Hz), 7.08 (2H, dd, J = 1.6, 7.5 Hz), 7.23 (3H, dd, J = 5.7, 9.3 Hz), 7.30 (1H, s); ^{13}C NMR (75 MHz, $CDCl_3$) δ 26.3, 26.5, 26.6, 32.8, 34.2, 34.8, 39.6, 42.3, 54.8, 62.2, 127.9, 128.8, 129.5, 140.6, 176.6; HRMS (ESI-TOF)$^+$ calcd for $C_{28}H_{44}N_4O_2$ (M + H)$^+$ 469.3543, found 469.3549. Anal. Calcd for $C_{28}H_{44}N_4O_2$: C, 71.76; H, 9.46; N, 11.95. Found: C, 71.38; H, 9.40; N, 11.87.

■ ASSOCIATED CONTENT

Ⓢ Supporting Information

^1H and ^{13}C NMR spectra as well as mass spectra for compounds **1-Boc**, **1**, and **2**; 2D NMR spectra for compounds **2**; and optimized *XYZ* geometries. This material is available free of charge via the Internet at http://pubs.acs.org.

■ AUTHOR INFORMATION

Corresponding Authors

*E-mail: luiss@qio.uji.es.

*E-mail: cativiela@unizar.es.

Notes

The authors declare no competing financial interest.

■ ACKNOWLEDGMENTS

S.V.L. acknowledges GV (PROMETEO/2012/020) and MINECO (CTQ2012-38543-C03-01). C.C. acknowledges

Ministerio de Ciencia e Innovación−FEDER (CTQ2010-17436) and Gobierno de Aragón−FSE (Research Group E40). V.M.-C. thanks MICINN for personal financial support (FPU Fellowship AP2007-02562). The support of the SCIC of the UJI for the different instrumental techniques is acknowledged.

REFERENCES

(1) Wessjohann, L. A.; Ruijter, E.; Garcia-Rivera, D.; Brandt, W. *Mol. Diversity* **2005**, *9*, 171−186.
(2) Wessjohann, L. A.; Ruijter, E. Strategies for Total and Diversity-Oriented Synthesis of Natural Product(-Like) Macrocycles. In *Natural Product Synthesis I*; Springer: Berlin, 2005; pp 137−184.
(3) Kubik, S. *Chem. Soc. Rev.* **2009**, *38*, 585−605.
(4) Kubik, S. Cyclopeptide Derived Synthetic Receptors. In *Artificial Receptors for Chemical Sensors*; Mirsky, V. M., Yatsimirsky, A. K., Eds.; Wiley-VCH: Weinheim, Germany, 2010; pp 135−167.
(5) Kubik, S. Synthetic Peptide-Based Receptors. In *Supramolecular Chemistry: From Molecules to Nanomaterials*; Gale, P. A., Steed, J. W., Eds.; John Wiley & Sons: Chichester, U.K., 2012; Vol. 3, pp 1179−1203.
(6) Blankenstein, J.; Zhu, J. *Eur. J. Org. Chem.* **2005**, 1949−1964.
(7) Wessjohann, L. A.; Ruijter, E. *Mol. Diversity* **2005**, *9*, 159−169.
(8) Bazzicalupi, C.; Bencini, A.; Bianchi, A.; Giorgi, C.; Paoletti, P.; Valtancoli, B.; Fusi, V.; Garcia-Españta, B. A.; Llinares, J. M. *J. Heterocycl. Chem.* **2001**, *38*, 1273−1279.
(9) White, C. J.; Yudin, A. K. *Nat. Chem.* **2011**, *3*, 509−524.
(10) Jiang, S.; Li, Z.; Ding, K.; Roller, P. P. *Curr. Org. Chem.* **2008**, *12*, 1502−1542.
(11) Davies, J. S. *J. Pept. Sci.* **2003**, *9*, 471−501.
(12) Lambert, J. N.; Mitchell, J. P.; Roberts, K. D. *J. Chem. Soc., Perkin Trans. 1* **2001**, 471−484.
(13) Laurent, B. A.; Grayson, S. M. *Chem. Soc. Rev.* **2009**, *38*, 2202−2213.
(14) Winnik, M. A. *Chem. Rev.* **1981**, *81*, 491−524.
(15) Ten Cate, A. T.; Kooijman, H.; Spek, A. L.; Sijbesma, R. P.; Meijer, E. W. *J. Am. Chem. Soc.* **2004**, *126*, 3801−3808.
(16) Huang, F.; Nau, W. M. *Angew. Chem., Int. Ed.* **2003**, *42*, 2269−2272.
(17) Marsault, E.; Peterson, M. L. *J. Med. Chem.* **2011**, *54*, 1961−2004.
(18) Gibson, S. E.; Lecci, C. *Angew. Chem., Int. Ed.* **2006**, *45*, 1364−1377.
(19) Luis, S. V.; Alfonso, I. *Acc. Chem. Res.* **2013**, DOI: 10.1021/ar400085p.
(20) Martí-Centelles, V.; Burguete, M. I.; Galindo, F.; Izquierdo, M. A.; Kumar, D. K.; White, A. J. P.; Luis, S. V.; Vilar, R. *J. Org. Chem.* **2012**, *77*, 490−500.
(21) Alfonso, I.; Burguete, M. I.; Galindo, F.; Luis, S. V.; Vigara, L. *J. Org. Chem.* **2007**, *72*, 7947−7956.
(22) Becerril, J.; Bolte, M.; Burguete, M. I.; Galindo, F.; García-España, E.; Luis, S. V.; Miravet, J. F. *J. Am. Chem. Soc.* **2003**, *125*, 6677−6686.
(23) Ramos, S.; Alcalde, E.; Doddi, G.; Mencarelli, P.; Pérez-García, L. *J. Org. Chem.* **2002**, *67*, 8463−8468.
(24) Martí-Centelles, V.; Burguete, M. I.; Luis, S. V. *Chem.—Eur. J.* **2012**, *18*, 2409−2422.
(25) Vilar, R. *Angew. Chem., Int. Ed.* **2003**, *42*, 1460−1477.
(26) Alcalde, E.; Ramos, S.; Pérez-García, L. *Org. Lett.* **1999**, *1*, 1035−1038.
(27) Revilla-López, G.; Warren, J. G.; Torras, J.; Jiménez, A. I.; Cativiela, C.; Alemán, C. *Biopolymers: Pept. Sci.* **2012**, *98*, 98−110.
(28) Solanas, C. N.; de la Torre, B. G.; Fernández-Reyes, M. A.; Santiveri, C. M.; Jiménez, M. A. N.; Rivas, L.; Jiménez, A. I.; Andreu, D.; Cativiela, C. *J. Med. Chem.* **2010**, *53*, 4119−4129.
(29) Frost, J. R.; Vitali, F.; Jacob, N. T.; Brown, M. D.; Fasan, R. *ChemBioChem* **2013**, *14*, 147−160.
(30) Wang, D.; Song, S.; Tian, Y.; Xu, Y.; Miao, Z.; Zhang, A. *J. Nat. Prod.* **2013**, *76*, 974−978.
(31) Fluxa, V. S.; Reymond, J.-L. *Bioorg. Med. Chem.* **2009**, *17*, 1018−1025.
(32) Flory, P. J.; Semlyen, J. A. *J. Am. Chem. Soc.* **1966**, *88*, 3209−3212.
(33) Winnik, M. A. *Acc. Chem. Res.* **1985**, *18*, 73−79.
(34) Halgren, T. A. *J. Comput. Chem.* **1996**, *17*, 490−519.
(35) Gutte, B. *Peptides: Synthesis, Structures, and Applications*; Elsevier Science: London, 1995.
(36) Martí-Centelles, V.; Burguete, M. I.; Luis, S. V. *Sci. World J.* **2012**, No. 748251.
(37) *Mathematica Software*; Wolfram Research, Inc.: Champaign, IL, 2008.
(38) Laidler, K. J.; King, M. C. *J. Phys. Chem.* **1983**, *87*, 2657−2664.
(39) Petersson, G. A. *Theor. Chem. Acc.* **2000**, *103*, 190−195.
(40) Fujita, Y.; Fujita, S.; Okada, Y.; Chiba, K. *Org. Lett.* **2013**, *15*, 1155−1157.
(41) Becerril, J.; Bolte, M.; Burguete, M. I.; Escorihuela, J.; Galindo, F.; Luis, S. V. *CrystEngComm* **2010**, *12*, 1722−1725.
(42) Becerril, J.; Burguete, M. I.; Escuder, B.; Galindo, F.; Gavara, R.; Miravet, J. F.; Luis, S. V.; Peris, G. *Chem.—Eur. J.* **2004**, *10*, 3879−3890.
(43) Laidler, K. J.; King, M. C. *J. Phys. Chem.* **1983**, *87*, 2657−2664.
(44) Truhlar, D. G.; Hase, W. L.; Hynes, J. T. *J. Phys. Chem.* **1983**, *87*, 2664−2682.
(45) Becke, A. D. *J. Chem. Phys.* **1993**, *98*, 5648−5652.
(46) Tomasi, J.; Persico, M. *Chem. Rev.* **1994**, *94*, 2027−2094.
(47) Tomasi, J.; Mennucci, B.; Cammi, R. *Chem. Rev.* **2005**, *105*, 2999−3094.
(48) Fukui, K. *Acc. Chem. Res.* **1981**, *14*, 363−368.
(49) Frisch, M. J.; Trucks, G. W.; Schlegel, H. B.; Scuseria, G. E.; Robb, M. A.; Cheeseman, J. R.; Scalmani, G.; Barone, V.; Mennucci, B.; Petersson, G. A.; Nakatsuji, H.; Caricato, M.; Li, X.; Hratchian, H. P.; Izmaylov, A. F.; Bloino, J.; Zheng, G.; Sonnenberg, J. L.; Hada, M.; Ehara, M.; Toyota, K.; Fukuda, R.; Hasegawa, J.; Ishida, M.; Nakajima, T.; Honda, Y.; Kitao, O.; Nakai, H.; Vreven, T.; Montgomery, J. A., Jr.; Peralta, J. E.; Ogliaro, F.; Bearpark, M.; Heyd, J. J.; Brothers, E.; Kudin, K. N.; Staroverov, V. N.; Kobayashi, R.; Normand, J.; Raghavachari, K.; Rendell, A.; Burant, J. C.; Iyengar, S. S.; Tomasi, J.; Cossi, M.; Rega, N.; Millam, J. M.; Klene, M.; Knox, J. E.; Cross, J. B.; Bakken, V.; Adamo, C.; Jaramillo, J.; Gomperts, R.; Stratmann, R. E.; Yazyev, O.; Austin, A. J.; Cammi, R.; Pomelli, C.; Ochterski, J. W.; Martin, R. L.; Morokuma, K.; Zakrzewski, V. G.; Voth, G. A.; Salvador, P.; Dannenberg, J. J.; Dapprich, S.; Daniels, A. D.; Farkas, Ö.; Foresman, J. B.; Ortiz, J. V.; Cioslowski, J.; Fox, D. J. *Gaussian 09*, revision B.01; Gaussian, Inc.: Wallingford, CT, 2009.
(50) Deppmeier, B. J.; Driessen, A. J.; Hehre, T. S.; Hehre, W. J.; Johnson, J. A.; Klunzinger, P. E.; Leonard, J. M.; Pham, I. N.; Pietro, W. J.; Jianguo, Y. *Spartan'08*, build 132 (Mar 27, 2009); Wavefunction, Inc.: Irvine, CA, 2009.